Long-Range Dipolar Couplings in Liquid Crystals Measured by Three-Dimensional NMR Spectroscopy

Stefano Caldarelli, Anne Lesage, and Lyndon Emsley*

Laboratoire de Stéréochimie et des Interactions Moléculaires UMR-117 CNRS/ENS, Ecole Normale Supérieure de Lyon 69364 Lyon, France

Received July 12, 1996

Liquid crystalline materials are of great biological and technological interest, but the formation, structure and stability of these mesophases is not yet fully understood. NMR methods have provided one of the most powerful tools for studying these phases at the molecular level through the measurement of average dipolar couplings.[1,2] For many years, dipolar couplings were obtained by analysis of one-dimensional (single- or multiple-quantum[3]) spectra, but at least in the absence of multidimensional techniques incorporating deuteration[4,5] or the use of dilute carbon pairs,[6,7] such an approach is limited to relatively simple systems. Recently, the introduction of two-dimensional techniques[8−14] for measuring heteronuclear dipolar couplings has extended the range of applications to more complex liquid crystalline molecules, such as phospholipids. Both 1D and 2D methods, however, provide accurate short-range (often one bond) dipolar couplings, but yield no reliable information on long-range couplings. In this paper we present a three-dimensional NMR experiment for measuring directly long-range heteronuclear dipolar couplings in anisotropic phases. The method is used to determine chain−chain, chain−core, and intercore dipolar couplings in the nematic liquid crystal 5CB (**1**).[15]

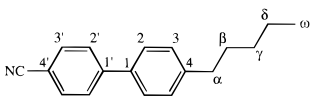

1

The pulse sequence for the experiment is shown in Figure 1a. It consists of a first evolution period of proton coherence during which homonuclear proton−proton dipolar couplings are removed by a MREV-8 (or equivalent) sequence.[16,17] A 180° pulse is applied simultaneously to the carbon and proton spins in the center of t_1 to refocus the proton chemical shift while retaining heteronuclear dipolar couplings, and thus the net evolution during t_1 is under the effect of only heteronuclear dipolar couplings. During the second evolution period, proton coherence precesses under only the effect of the proton chemical shift, with the homonuclear couplings being removed by MREV-8 and the heteronuclear couplings being refocused by a 180° carbon pulse at the center of t_2. This period is followed by cross polarization to carbon and detection of the carbon free-induction decay in the presence of proton decoupling. The resulting spectrum after 3D Fourier transformation yields a *pairwise dipolar field spectrum*, as illustrated in Figure 1b, where for each distinguishable carbon−proton pair in the $\omega_3-\omega_2$ correlation plane, the ω_1 line contains a single doublet splitting which represents the averaged dipolar coupling between the two nuclei. Note that a doublet splitting is observed irrespective of the multiplicity of the proton[11,13] (CH, CH_2, or CH_3) because we measure the proton spectrum in ω_1 (split by the H−C dipolar coupling) rather than measuring the carbon spectrum in ω_1.

For 5CB, all of the carbon resonances are resolved and the dipolar decoupled proton spectrum has peaks corresponding to the ω proton, the δ, γ, and β protons (degenerate), the α proton, the 2, 3, and 2′ protons (degenerate), and the 3′ proton. At this level of resolution we are able to measure unambiguously the chain−chain couplings between the Hω and the ω, δ, γ, and β

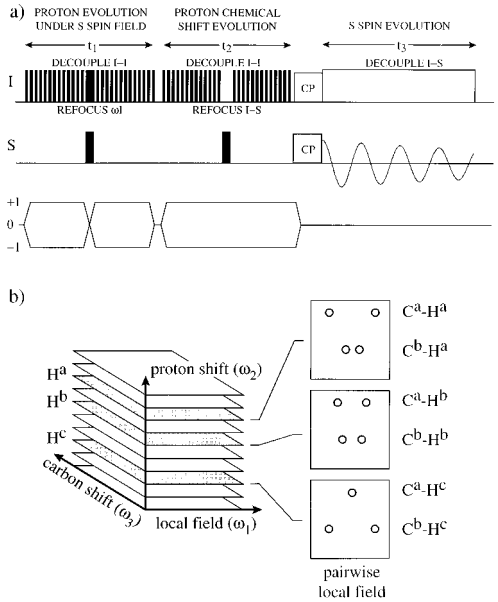

Figure 1. (a) Pulse sequence suitable for pairwise local field spectroscopy. Coherence is excited by a 90° pulse followed by a 45° "prepulse" before the MREV-8 sequence. A second 45° pulse after the sequence stores one component of the magnetization along the *z* axis (allowing States or TPPI type acquisition of both $p = \pm 1$ coherences in t_1). The magnetization is recalled by a further 90−45° sequence before t_2 and the application of the second MREV-8 cycle. At the end of t_2, a 45° pulse aligns the magnetization along the *y* axis before the cross polarization step transfers this component to the carbon spins (allowing States or TPPI type acquisition of both $p = \pm 1$ coherences in t_2). The wide pulses at the center of t_1 and t_2 represent 180° pulses. An 8-step phase cycle is employed to select the coherence transfer pathway for the protons shown below the sequence. Note that the carbon 180° pulse in t_2 could be replaced by continuos decoupling throughout t_2 and that the MREV-8 sequences could be replaced by other homonuclear dipolar decoupling sequences with suitable prepulses. The pulse program used to acquire spectra is available on request from the authors. In b we show schematically the pairwise local field spectrum that results after 3D Fourier transformation.

* Author to whom correspondence should be addressed.

(1) *Nuclear Magnetic Resonance of Liquid Crystals*; Emsley, J. W., Ed.; Reidel: Dordrecht, The Netherlands, 1985.
(2) Dong, R. Y. *Nuclear Magnetic Resonance of Liquid Crystals (Partially Ordered Systems)*; Springer-Verlag: Berlin, 1994.
(3) Sinton, S. W.; Zax, D. B.; Murdoch, J. B.; Pines, A. *Mol. Phys.* **1984**, *53*, 333.
(4) Gochin, M.; Schenker, K. V.; Zimmerman, H.; Pines, A. *J. Am. Chem. Soc.* **1986**, *108*, 6813.
(5) Gochin, M.; Zon, G.; James, T. L. *Biochemistry* **1990**, *29*, 11161.
(6) Sandström, D.; Summanen, K. T.; Levitt, M. H. *J. Am. Chem. Soc.* **1994**, *116*, 9357.
(7) Sandström, D.; Levitt, M. H. *J. Am. Chem. Soc.* **1996**, *118*, 6966.
(8) Fung, B. M.; Afzal, J. *J. Am. Chem. Soc.* **1986**, *108*, 1107.
(9) Fung, B. M.; Afzal, J. *J. Chem. Phys.* **1986**, *85*, 4808.
(10) Courtieu, J.; Bayle, J. P.; Fung, B. M. *Prog. NMR Spectrosc.* **1994**, *26*, 141.
(11) Schmidt-Rohr, K.; Nanz, D.; Emsley, L.; Pines, A. *J. Phys. Chem.* **1994**, *98*, 6668.
(12) Hong, M.; Schmidt-Rohr, K.; Nanz, D. *Biophys. J.* **1995**, *69*, 1939.
(13) Caldarelli, S.; Hong, M.; Emsley, L.; Pines, A. *J. Phys. Chem.* In press.
(14) Hong, M.; Caldarelli, S.; Schmidt-Rohr, K.; Pines, A. *J. Phys. Chem.* **1996**, *100*, 14815.
(15) 4-*n*-Pentyl-4′-cyanobiphenyl was obtained from Aldrich Chemical Co. and used without further purification.
(16) Mansfield, P. *J. Phys. C* **1971**, *4*, 1444.
(17) Rhim, W. K.; Elleman, D. D.; Vaughan, R. W. *J. Chem. Phys.* **1972**, *58*, 1772.

S0002-7863(96)02393-1 CCC: $12.00

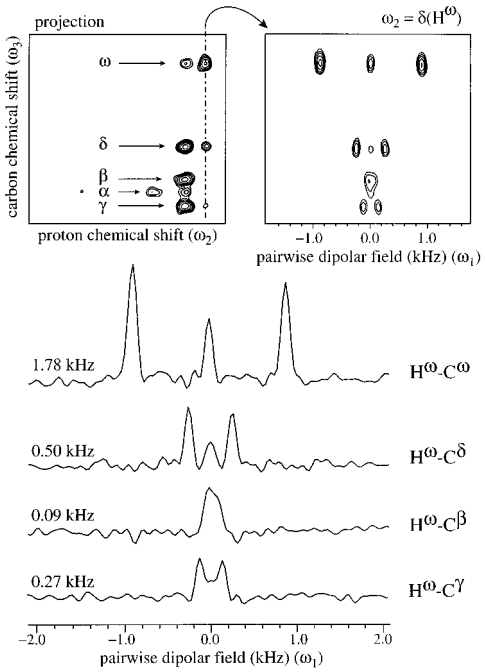

Figure 2. The aliphatic region of the 3D pairwise local field spectrum of the nematic liquid crystal 5CB. A projection onto the $\omega_2-\omega_3$ plane yields a carbon−proton shift correlation spectrum (upper left), and a plane taken perpendicular to this at a particular proton chemical shift (upper right) yields a $\omega_3-\omega_1$ slice that contains a series of pairwise local fields for each carbon atom. In the figure, we show the pairwise local fields obtained for Hω and observe that we can simply measure the Hω couplings to the carbons all the way down the chain to Cβ. For Cβ, the value of 0.09 kHz was obtained from a fit of the line shape assuming the line shape observed in the other traces (one can immediately see that this trace represents a nearly resolved splitting). The spectrum was recorded at room temperature at a proton frequency of 500 MHz on a Varian Unity+ spectrometer using a narrow-bore double-tuned MAS probe (without sample rotation). The 90° proton pulse width was 4.3 μs and the MREV-8 cycle time was 63.6 μs, leading to an effective spectral width of 8.4 kHz in ω_1 including correction for the MREV-8 scaling factor (0.47). The signal was sampled every other cycle in ω_2, leading to a spectral width of 4.2 kHz. Eight scans were recorded for each of 64 increments in t_1 and 40 increments in t_2. The data were zero-filled to 512 × 256 × 1024 before apodisation with a Gaussian function in each dimension and Fourier transformation. The spectra are phase sensitive and were obtained with the States method of sign discrimination in t_1 and t_2. The cross polarization time was relatively long (2 ms) to favor long-range transfer. Since we have no active temperature control, a 4.0 s recycle delay was used between scans to avoid problems associated with sample heating. Note, that it is probable that with higher radiofrequency (rf) powers, shorter pulses, and active temperature control even better resolution can be obtained than that obtained here with very modest 90° pulse widths. For example, the presence of the weak peak in the center of the spectrum is a reflection of an error associated with the 45° prepulses and the MREV-8 sequence.

carbons, as shown (with the measured values) in Figure 2. Previous 2D PDLF (proton detected local field) measurements have only been able to unambiguously identify the Hω−Cω coupling.[13] We can similarly measure couplings between Hα and the aliphatic carbons, and perhaps more importantly we observe a 1.1 kHz splitting between Hα and the aromatic C3. Finally, we observe a 0.25 kHz coupling between H3′ and C2, establishing a link between the two aromatic rings. The measurement of long-range couplings is particularly important

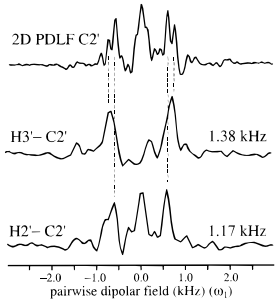

Figure 3. The pairwise local fields obtained for H3′-C2′ and H2′-C2′ in the nematic liquid crystal 5CB. The spectra are compared with the C2′ trace from a 2D PDLF experiment[13] and demonstrate how the 3D experiment allows the assignment of the two couplings, which is not possible in the 2D experiment. We note that the one-bond H2′-C2′ splitting is the smaller of the two. The 3D spectrum was recorded under the same conditions as that used in Figure 2, except that the cross polarization time was 500 μs. The 90° proton pulse width was 4.5 μs, and the MREV-8 cycle time was 66 μs, leading to a spectral width of 8.0 kHz in ω_1 including correction for the MREV-8 scaling factor (0.47). The signal was sampled every other cycle in ω_2, leading to a spectral width of 4.0 kHz. Eight scans were recorded for each of 40 increments in t_1 and 40 increments in t_2. The 2D spectrum has a higher resolution because 128 points were acquired in t_1, and a lighter apodisation function was used during processing.

since they provide particularly strong experimental constraints for models of the internal motions of these molecules in the nematic phase. The chain−chain interactions constrain the chain dynamics, the chain−core interactions constrain the relative orientation of the chain with respect to the aromatic core, and the interactions between the aromatic rings constrain the relative orientation of the two rings. None of these long-range interactions have previously been measured.

Note that, apart from the measurement of long-range splittings, the method also allows the assignment of short- and medium-range splittings, which is not possible in 2D experiments. Figure 3 demonstrates this for the couplings to C2′. In the 2D PDLF experiment, one observes two splittings similar in magnitude, and it is tempting to conclude that the larger splitting corresponds to the H2′−C2′ coupling, on the basis of spatial proximity, and the smaller coupling to the H3′−C2′ splitting. The pairwise local field spectra shown in the figure demonstrate that without any doubt the couplings are in fact inverted and that, due to the orientational dynamics of the molecule, the averaged H2′−C2′ splitting is the smaller of the two.

In conclusion, the 3D pairwise local field spectroscopy method presented here has allowed us, for the first time, to measure and assign directly long-range dipolar couplings in oriented phases without any geometrical assumptions. It is also the first time a three-dimensional technique has been used in a liquid crystal. We have demonstrated the method on a model single-component nematic liquid crystal, and even in this well-characterized system,[18,19] we have been able to provide data that was previously unavailable. The technique should be equally applicable to measure heteronuclear couplings in lipid samples, multicomponent liquid crystals, or liquid crystals in cholesteric or ferroelectric phases.

JA9623931

(18) Emsley, J. W.; Luckhurst, G. R.; Stockley, C. P. *Mol. Phys.* **1981**, *44*, 565.
(19) Photinos, D. J.; Samulski, E. T.; Toriumi, H. *J. Chem. Phys.* **1991**, *94*, 2758.